The Astrophysical Journal, 906:81 (6pp), 2021 January 10 https://doi.org/10.3847/1538-4357/abc5c5
© 2021. The American Astronomical Society. All rights reserved.

Lorentz–Lorenz Coefficient of Ice Molecules of Astrophysical Interest: N_2, CO_2, NH_3, CH_4, CH_3OH, C_2H_4, and C_2H_6

M. Domingo, R. Luna, M. Á. Satorre, C. Santonja, and C. Millán
Centro de Tecnologías Físicas, Universitat Politècnica de València, Plaza Ferrándiz-Carbonell, E-03801 Alcoy, Spain; mdomingo@fis.upv.es
Received 2019 February 28; revised 2020 October 25; accepted 2020 October 27; published 2021 January 11

Abstract

This work calculates the Lorentz–Lorenz coefficient with the refractive index and density values of various molecules in their solid phase measured in our laboratory under astrophysical conditions. This was completed for a range of temperatures from 13 K to close to the sublimation temperature for each molecule. The studied molecules were N_2, CO_2, NH_3, CH_4, CH_3OH, C_2H_4, and C_2H_6. For CO_2, our results match those found in the unique similar previous work in the literature. The results obtained for NH_3 and CH_3OH are relevant because they confirm that the procedure adopted is applicable also to polar molecules. The study presented here updates the previous work on these molecules by focusing on their solid states under astrophysical conditions and at a range of temperatures. The knowledge of the Lorentz–Lorenz coefficient in a specific temperature range allows for calculating the density using only the refractive index.

Unified Astronomy Thesaurus concepts: Laboratory astrophysics (2004); Solid matter physics (2090); Matter density (1014); Interstellar molecules (849); Interstellar abundances (832); Surface ices (2117)

1. Introduction

The molecules studied in this work are present in different astrophysical scenarios that are cold enough to form their ices. These environments include icy mantles in dense interstellar clouds (Lacy et al. 1991, 1998; Gerakines et al. 1999), young stellar objects (Gibb et al. 2004), planets and satellites in the solar system (Brown et al. 1995; Brooke et al. 1998; Mousis & Alibert 2006), and trans-Neptunian objects (Dotto et al. 2003). The physical conditions in these scenarios vary widely and the variables representing their state, such as density, might also vary. Therefore, laboratory experiments that attempt to reproduce such conditions should be performed over a wide range of temperatures.

When possible, experimental astrophysics laboratories often use several techniques simultaneously during the same experiment to obtain as much experimental data as possible from the ice under study. These techniques usually include IR, UV, and/or visible spectroscopy to study the absorption bands that characterize the molecules of which the ice is composed (Moore & Hudson 2010; Hudson et al. 2014; Drobyshev et al. 2019), interferometry with two lasers to determine the refractive index and thickness of the ice (Romanescu et al. 2010; Satorre et al. 2013; Drobyshev et al. 2017), quartz crystal microbalance techniques to measure the mass of the ice and the desorption energy (Luna et al. 2014), mass spectrometer measurements to detect the components of the ice during desorption or thermal programmed desorption experiments (Collings et al. 2004; Luna et al. 2012), and UV lamp (Gerakines et al. 1996; Muñoz Caro et al. 2019) or ion gun (Brunetto et al. 2006; Hudson & Moore 2018) experiments to examine the energetic processing of the ice. When this is not possible, it is common to use bibliographic results if intensive data are needed, such as for density and refractive index. This alternative presents the disadvantage that these values have not always been measured in experiments under the same conditions as those of the group interested in them or may not even be available.

Density values for ices under astrophysical conditions are scarce in the literature. They are used to obtain band strengths of molecules of astrophysical interest (Hudson et al. 2014), which allows for the calculation of their abundance from observational spectra (Yamagishi et al. 2011), to estimate the penetration depth of energetic ions in simulations of energetic ice processing (Srim Software[1]), and to establish ice buoyancy hypotheses (Roe & Grundy 2012).

The refractive index is a fundamental property of matter in its interaction with electromagnetic waves. In astrophysics, knowledge of the refractive index is essential to extract information from observations as well as to investigate the structure of matter and take measurements of other magnitudes.

These two elemental magnitudes, refractive index and density, can be related to each other when quite general conditions are met, as a perfect order or disorder of the molecules. This relationship is the Lorentz–Lorenz approximation, originally developed for nonpolar molecules (Born & Wolf 1999), which relates parameters that macroscopically characterize an ice, such as density, ρ, and refractive index, n, to the polarizability, α, which is associated with the properties of the molecule. Its expression in the International System is

$$\frac{n^2-1}{n^2+2}=\frac{10^{-24}N_A 4\pi\alpha}{3M}\rho, \tag{1}$$

where N_A is Avogadro's number; M is the molar mass in g mol^{-1}; density, ρ, is in g cm^{-3}; and α in Å^3 is the polarizability volume.

If there is no change in the rovibrational state of the molecule in the temperature range studied, the polarizability, which is proportional to the size of the molecule, will remain constant (Guella et al. 1991; Miller 2009) and Equation (1) can be written as

$$\frac{n^2-1}{n^2+2}=L\cdot\rho, \tag{2}$$

[1] http://www.srim.org/

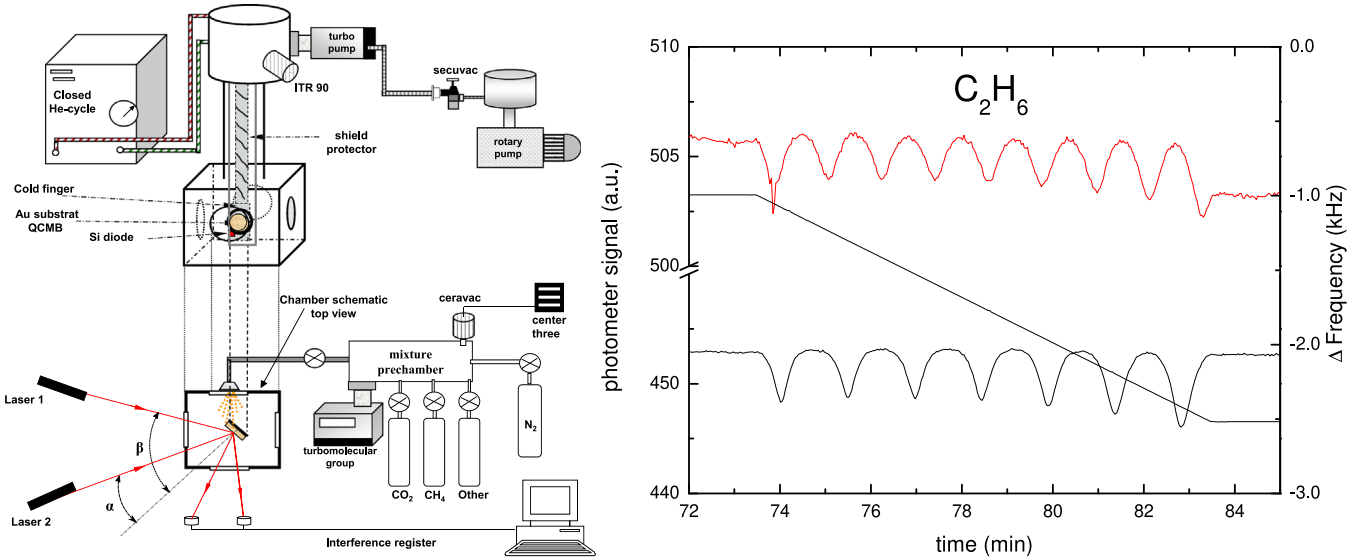

Figure 1. (a) Scheme of the experimental apparatus and (b) plot from a C_2H_6 deposition experiment at $T = 35$ K: the interference curves of each laser beam from the photometer signals ($\alpha = 33.^{\circ}6$ in red, $\beta = 66.^{\circ}1$ in black) and the variation of the frequency of the QCMB (the solid line with a constant slope).

where L is the Lorentz–Lorenz coefficient or factor (Guenther 2015) in $cm^3\ g^{-1}$.

If the Lorentz–Lorenz approximation is valid and the Lorentz–Lorenz factor, L, is known, ρ can be obtained using values of n from experiments or from the bibliography. For example, Brunetto et al. (2008) took L from Roux et al. (1980) and with the n measured with their experiments, they obtained ρ. This is the main utility in knowing L.

Some authors have measured polarizability values in gas-phase experiments under different conditions for temperature (in general, with only a single value) and pressure (much larger than a high vacuum, such as atmospheric pressure or greater) with either a static electric field or a dynamic field from an electromagnetic wave. In these works, the density is not always measured under the same conditions as the refractive index, but its value is usually extrapolated using an equation of state. The refractive index has been measured by the change in the resonant frequency of a chamber filled with the substance under study (Newell & Baird 1965) as well as by the difference in the capacitance of a capacitor when empty or filled with the substance (Orcutt & Cole 1967; Bose & Cole 1970, 1971; Bose et al. 1972).

Other authors have performed solid-phase experiments in high vacuum and low-temperature conditions. Roux et al. (1980) obtained L for several molecules by measuring n and ρ at a single temperature (20 K). Loeffler et al. (2016) performed a linear fitting with the experimental data of n and ρ for CO_2 for a range of temperatures, and the authors take the slope as the Lorentz–Lorenz coefficient L. Aldiyarov et al. (2017) have obtained the polarizability value of methane in the range of 14–30 K, concluding that it varied. All of them have measured the refractive index through interferometry with one or two lasers and the mass deposited with a quartz microbalance (Roux et al. 1980; Loeffler et al. 2016) or with the equation of perfect gases from a calibrated quantity of gas (Aldiyarov et al. 2017).

2. Experimental Setup

The experiments were performed following a setup described in detail in previous works (Satorre et al. 2008 and Satorre et al. 2013). It consists, as shown in Figure 1(a), of a high vacuum chamber at a base pressure of 10^{-7} mbar that is obtained by evacuating continuously with a Leybold TurboVac 50 turbomolecular pump backed with a Leybold Trivac 1.6B rotary mechanical pump and measured with a Leybold ITR 90 IONIVAC transmitter. Inside the chamber is a sample holder that can be cooled to 10 K by a closed-cycle He cryostat that operates according to the Gifford–McMahon principle.

The temperature of the sample holder can be controlled by an Oxford ITC 503S temperature controller to go from 10 K to room temperature with 0.5 K accuracy. It measures the temperature using a silicon diode (Scientific Instruments Model 1901) and heat can be delivered to the sample holder at a controlled intensity by a resistor connected to the end of the second stage of the He cycle. Above the sample holder, in thermal contact with it, is a gold-plated quartz crystal microbalance (QCMB; 5 MHz AT-cut Q-Sense). When the desired pressure and temperature conditions are achieved, the chamber is filled with gas molecules, which come from a prechamber through a Leybold variable-leak needle valve. The molecules then freeze onto the gold electrode of the QCMB when they collide with it from all directions (background deposition).

A constant rate of deposition is the cornerstone of the method used in this study. Approximate values for the molecules were, in $\mu m/h$: 2.1 for N_2, 2.4 for CO_2, 1.2 for NH_3, 0.5 for CH_4, 4.3 for CH_3OH, and between 1 and 15 for C_2H_4 and C_2H_6. In order to achieve the constant rate of deposition, a capacitive sensor element (CERAVAC CTR 90), connected to a CENTER THREE vacuum gauge controller to ensure a precision better than 0.2% during deposition, controls the pressure in the prechamber.

Before each experiment, the prechamber is evacuated using a turbomolecular group pump. A gate valve with a toggle lever

(VAT Vakuumventile AG, CH 9469) isolates the high vacuum part of the system. After a pressure lower than 10^{-4} mbar is achieved, the aluminum prechamber is isolated from the pressure group with a pressure gate valve similar to the one used before and then it is ready to be filled with gas.

During the deposition of the gas on the QCMB, we obtain two interferograms of two polarized (perpendicular to the plane of incidence) He–Ne lasers (Figure 1(b)) from two BPW21 photodiodes. As the thickness and the refractive index are the same for both interference patterns and the incidence angles α and β are known, we can calculate the refractive index as it is described in Tempelmeyer & Mills (1968) using Equation (3):

$$n^2 = \frac{\sin^2\beta - \gamma^2 \sin^2\alpha}{1 - \gamma^2}, \tag{3}$$

where $\gamma = \frac{T_\alpha}{T_\beta}$ and T_α and T_β are the periods of the interference curves for the corresponding angles of incidence.

Knowing the refractive index and counting the number of interference curves for one of the lasers, q_α or q_β, the thickness d of the ice is calculated using Equation (4):

$$d = q_\alpha \frac{\lambda}{2n\sqrt{1 - \frac{\sin^2\alpha}{n^2}}} = q_\beta \frac{\lambda}{2n\sqrt{1 - \frac{\sin^2\beta}{n^2}}}, \tag{4}$$

where $\lambda = 632.8$ nm is the wavelength of the laser.

The constant rate of deposition is checked using the periods of both lasers and with the QCMB signal as well. By plotting the frequency versus time during the deposition of the gas, a linear decrease is obtained (Figure 1(b)). The Sauerbrey equation, Equation (5), relates these parameters:

$$\Delta f = -S \cdot \Delta m, \tag{5}$$

where Δf is the change in frequency, Δm represents the mass of the gas accreted onto the QCMB, and S is a specific constant for every QCMB system.

The samples are typically a few microns (μm) in thickness. The density is calculated by dividing the mass deposited per unit area (g cm^{-2}) measured with the QCMB from Equation (5) by the thickness (cm) determined by Equation (4).

We select deposition temperatures from the lowest value reachable on the QCMB to the closest temperature of sublimation for each molecule under high vacuum conditions.

The sources of errors come from the experimental measurements. In this case, these measurements are the angles of incidence, the constancy of periods during deposition, and the mass determination. The error values obtained were as follows: 0.4% for the angles of incidence, 1% for the periods, and 0.5% for the mass accreted. Using the propagation error theory, the final errors were 2.5% for the refractive index and 5% for the density.

3. Results and Discussion

The density ρ and the refractive index n values obtained in our laboratory for the molecules studied (Figure 2) have been presented in previous works: N_2, CO_2, and CH_4 in Satorre et al. (2008) (updated for CO_2 in Satorre et al. 2018); NH_3 in Satorre et al. (2013); CH_3OH in Luna et al. (2018); and C_2H_4 and C_2H_6 in Satorre et al. (2017). The results presented for CO_2 are the average of those from 2008 and new experiments performed from 2008 to 2018 using the same experimental apparatus and procedure. For N_2 and CH_4, the density and refractive index values are constant within the error range for the different deposition temperatures while for the rest (CO_2, NH_3, CH_3OH, C_2H_4, and C_2H_6), they increase with the temperature of deposition and eventually reach a plateau. For each ice, there is a limit on the temperature of deposition, which is when desorption starts. We assume that the variation of n and ρ with temperature is related to changes in the structure of the ice.

If we represent the experimental data from Figure 2 in the form $\frac{n^2-1}{n^2+2}$ versus ρ (Figure 3), we can see that for each molecule, all of the data are roughly in a straight line, which would confirm the situation that polarizability remains constant. Figure 3 shows that molecules are distributed into three zones: apolar hydrocarbons on the left, polar molecules in the center, and apolar molecules on the right.

Table 1 shows the result of applying Equation (2) to our experimental data and previous values from the bibliography. When we follow Equation (2) for each n_i and ρ_i at temperature T_i, we obtain L_i and take the average of L_i as the value of L, considering the uncertainty of this estimation as the semiamplitude of the 95% confidence interval (Student's t-distribution). In Figure 3, the line corresponding to Equation (2) has been drawn for each molecule with the values of L presented in Table 1. According to the error values for L and the fact that, for each molecule, this line passes through the areas delimited by the error bars in the experimental data, it can be deduced that Equation (2) is fulfilled.

Of all the molecules considered, only NH_3 and CH_3OH are polar (Atkins & de Paula 2006), but despite this, their results do not stand out from the others.

The values from the bibliography have generally been calculated at a single temperature (except for Loeffler et al. 2016 with CO_2) and in a gaseous state (except for Roux et al. 1980 with N_2 and CH_4, Wood & Roux 1982 with CO_2 and NH_3, and Loeffler et al. 2016 with CO_2). The last column of Table 1 shows the difference in percentage between the bibliographic values and our results.

Our L result for N_2 is closer to that of Newell & Baird (1965) and of Orcutt & Cole (1967) (with an 8.3% difference for both), obtained in the gas phase, than that of Roux et al. (1980) (with a 34% difference), obtained in the solid phase in similar conditions to ours, but at a single temperature of 20 K. For CO_2, our result differs only 5% with Loeffler et al. (2016), which performed the experiments in the solid phase at a range of temperatures; the difference with Wood & Roux (1982) (in the solid phase at 20 and 80 K) is 9% and with Bose & Cole (1970) (in the gas phase at 302.5 K) is 18%. For CH_4, our result is similar to that of Bose et al. (1972) (a 4% difference), obtained in the gaseous phase, but the difference is higher (28%) with the result of Roux et al. (1980) for the solid phase and very different from that of Aldiyarov et al. (2017), who measured that the polarizability varies in the temperature range investigated here.

For NH_3, our results match Le Fevre & Russell (1947) (a 1% difference) but not Barnes et al. (1971) (a 26% difference), who perform their experiments in the gas phase, and are similar to Wood & Roux (1982) (a 14% difference) in the solid phase at 20 and 80 K. For CH_3OH, C_2H_4, and C_2H_6, the differences are similar (around 15%) with the bibliography (from the gas phase), although there is a great coincidence (a 2% difference) with Ramaswamy (1935) for CH_3OH.

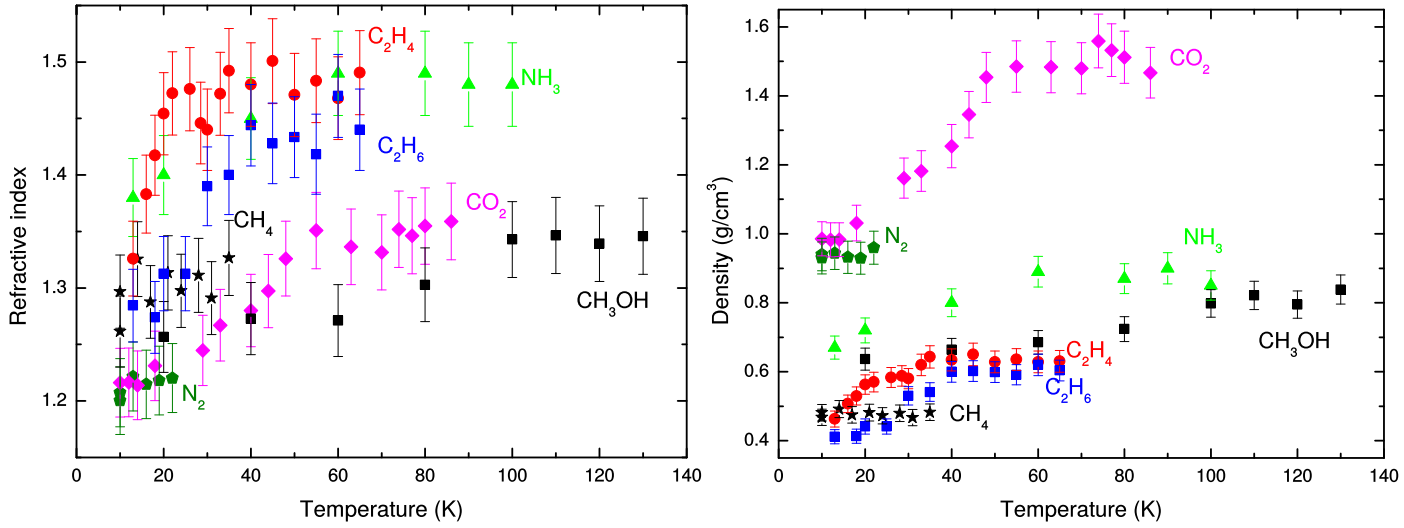

(a) (b)

Figure 2. Experimental data from the measurements of (a) the refractive index and (b) the density.

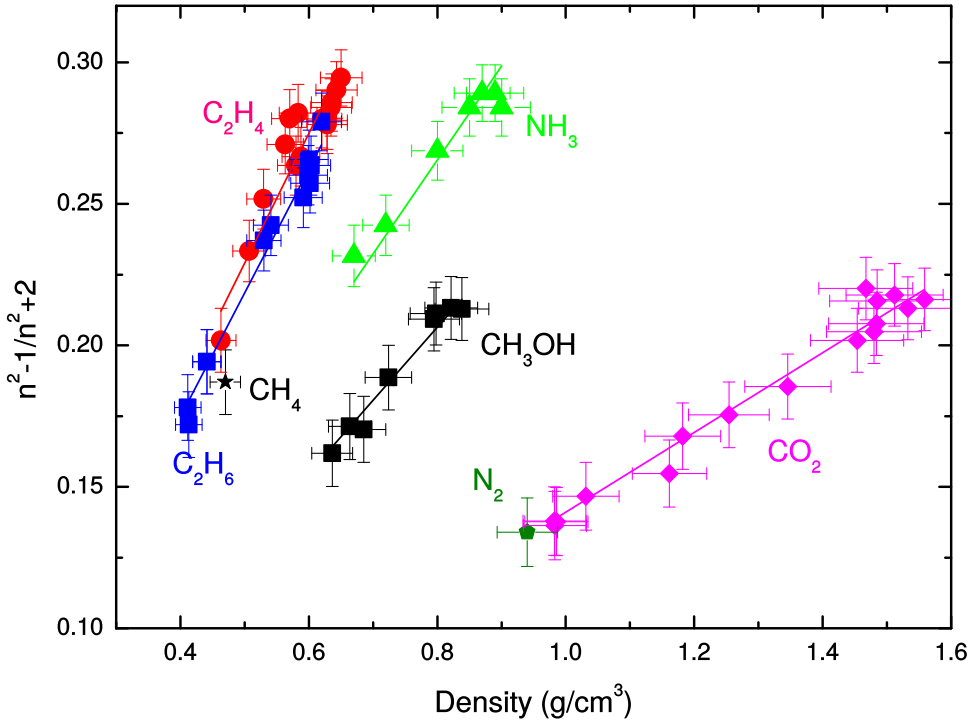

Figure 3. $\frac{n^2-1}{n^2+2}$ vs. ρ from our experimental data.

4. Conclusions

When the Lorentz–Lorenz approximation is satisfied by the ice of a molecule in a given temperature range, the Lorentz–Lorenz coefficient, L, can be used to obtain its density from its refractive index as well as its polarizability value, which will be constant in the range of temperatures studied.

In this article, we have calculated the Lorentz–Lorenz factor, L, for pure ices of N_2, CO_2, NH_3, CH_4, CH_3OH, C_2H_4, and C_2H_6, in the temperature range from deposition at 10 K to near desorption. This was accomplished by using our experimental data with Equation (2) (with an arithmetic mean). The values for L obtained are acceptable according to Figure 3 and the error values of L shown in Table 1. In the case of CO_2 ice, there is a very good agreement with Loeffler et al. (2016). Comparing our data to the literature values in Table 1, the maximum deviation of L, 34%, was found for solid N_2 in Roux et al. (1980). The maximum deviation of our ice data from the gas-phase values corresponds to NH_3, 26% compared to Barnes et al. (1971), but this deviation is negligible, 1%, compared to Le Fevre & Russell (1947). We found that the conclusions from Loeffler et al. (2016) for CO_2 can be extended to the other ice components, i.e., the method used for ice deposition influences the ice amorphicity and the value of the refractive index, but the Lorentz–Lorenz approximation is still fulfilled.

Table 1
The Values for the Lorentz–Lorenz Factor, L, for the Experimental Data Obtained in Our Laboratory According to Equation (2) and from the Bibliography

Molecule	Reference	Temp. (K) Phase	L ($cm^3 \cdot g^{-1}$)	% Difference
N_2	Satorre et al. (2008)	10–22 Solid	0.145 ± 0.011	⋯
	Roux et al. (1980)	20 Solid	0.194	34
	Newell & Baird (1965)	273.1 Gas	0.157	8.3
	Orcutt & Cole (1967)	322 Gas	0.157	8.3
CO_2	Satorre et al. (2008)	10–86 Solid	0.141 ± 0.002	⋯
	Loeffler et al. (2016)	14–70 Solid	0.148	5
	Wood & Roux (1982)	20, 80 Solid	0.155	9
	Bose & Cole (1970)	302.5 Gas	0.167	18
NH_3	Satorre et al. (2013)	13–100 Solid	0.332 ± 0.010	⋯
	Wood & Roux (1982)	20, 80 Solid	0.291	−14
	Barnes et al. (1971)	278.2, 298.2, 318.2 Gas	0.417	26
	Le Fevre & Russell (1947)	294–419 Gas	0.335	1
CH_4	Satorre et al. (2008)	10–35 Solid	0.393 ± 0.019	⋯
	Roux et al. (1980)	20 Solid	0.505	28
	Bose et al. (1972)	279.8, 322.5, 373.4 Gas	0.409	4
CH_3OH	Luna et al. (2018)	20–130 Solid	0.258 ± 0.005	⋯
	Kubo (1935)	308–482 Gas	0.303	17
	Ramaswamy (1935)	302, 368 Gas	0.253	−2
C_2H_4	Satorre et al. (2017)	13–60 Solid	0.458 ± 0.010	⋯
	Bose & Cole (1971)	323.1, 373.1, 423.1 Gas	0.383	−16
C_2H_6	Satorre et al. (2017)	13–60 Solid	0.437 ± 0.007	⋯
	Watson et al. (1934)	193, 298 Gas	0.372	−15

Note. The last column shows the difference in percentage from our L.

The Lorentz–Lorenz approximation (Equation (2)) is not the result of an exact theory that explains the relationship between the physical quantities involved. The simplifications introduced by the model led to the consideration that the electric field experienced by a molecule is $\vec{E} + \frac{\vec{P}}{3}$, where $\vec{E}$ is the macroscopic electrical field and $\vec{P}$ is the dipolar moment per unit volume (Panofsky & Phillips 1962). As these simplifications become less certain (e.g. due to high-density values, molecules of anomalous form, an unsuitable order or disorder, etc.), their validity diminishes and a corrective term may need to be introduced (Brillouin 1960; Stone 1963; Born & Wolf 1999). But the value of this corrective term is low and the fit of our data with the Lorentz–Lorenz approximation is reasonable without this correction.

Based on our results, we have determined that the Lorentz–Lorenz approximation applies to solids formed by the molecules we consider in this study over the entire range of temperatures (of astrophysical relevance) studied. Among the molecules we consider, there are two polar molecules: NH_3 and CH_3OH. So, we have demonstrated that the Lorentz–Lorenz approximation is also applicable to those polar molecules (Born & Wolf 1999).

Our coefficients from Table 1 are valuable because they allow calculating actual density values from refractive indices under astrophysical conditions in the indicated range of temperature. The measurements of parameters that depend on the density can thereby also be improved, such as the band strengths of molecules and, therefore, their abundances in observational spectra, the penetration depths of energetic ions, and ice buoyancy.

References

Aldiyarov, A., Drobyshev, A., Sokolov, D., & Shinbayeva, A. 2017, JLTP, 187, 749
Atkins, P., & de Paula, J. 2006, Atkins Physical Chemistry (8th ed.; Oxford: Oxford Univ. Press)
Barnes, A. N. M., Turner, D. J., & Sutton, L. E. 1971, Trans. Faraday Soc., 67, 2902
Born, M., & Wolf, E. 1999, Principles of Optics (Cambridge: Cambridge Univ. Press)
Bose, T. K., & Cole, R. H. 1970, JChPh, 52, 140
Bose, T. K., & Cole, R. H. 1971, JChPh, 54, 4033
Bose, T. K., Sochanski, J. S., & Cole, R. H. 1972, JChPh, 57, 3592
Brillouin, L. 1960, Wave Propagation and Group Velocity (New York: Academic)
Brooke, T. Y., Knacke, R. F., Encrenaz, Th., et al. 1998, Icar, 136, 1
Brown, R. H., Cruikshank, D. P., Veverka, J., Helfenstein, P., & Eluszkiewicz, J. 1995, Neptune and Triton (Tucson, AZ: Univ. of Arizona Press)
Brunetto, R., Barucci, M. A., Dotto, E., & Strazzulla, G. 2006, ApJ, 644, 646
Brunetto, R., Caniglia, G. A., Baratta, G. A., & Palumbo, M. E. 2008, ApJ, 686, 1480
Collings, M. P., Anderson, M. A., Chen, R., et al. 2004, MNRAS, 354, 1133
Dotto, E., Barucci, M. A., & de Bergh, C. 2003, Physique, 4, 775
Drobyshev, A., Aldiyarov, A., Sokolov, D., Shinbayeva, A., & Nurmukan, A. 2019, LTP, 45, 441
Drobyshev, A., Aldiyarov, A., Sokolov, D., Shinbayeva, A., & Tokmoldin, N. 2017, LTP, 43, 214
Gerakines, P. A., Schutte, W. A., & Ehrenfreund, P. 1996, A&A, 312, 289
Gerakines, P. A., Whittet, D. C. B., Ehrenfreund, P., et al. 1999, ApJ, 522, 357
Gibb, E. L., Whittet, D. C. B., Boogert, A. C. A., & Tielens, A. 2004, ApJS, 151, 35
Guella, T., Miller, T. M., Stockdale, J. A. D., Bederson, B., & Vuskovic, L. 1991, JChPh, 94, 6857
Guenther, B. D. 2015, Modern Optics (Oxford: Oxford Univ. Press)
Hudson, R. L., Gerakines, P. A., & Moore, M. H. 2014, Icar, 243, 1148
Hudson, R. L., & Moore, M. H. 2018, ApJ, 857, 89
Kubo, M. 1935, Sci. Papers Inst. Phys. Chem. Res., 27, 65
Lacy, J. H., Carr, J. S., Evans, N. J., II, et al. 1991, ApJ, 376, 556

Lacy, J. H., Faraji, H., Sandford, S. A., & Allamandola, L. J. 1998, ApJ, 376, 556
Le Fevre, R. J. W., & Russell, P. 1947, Trans. Faraday Soc, 43, 374
Loeffler, M. J., Moore, M. H., & Gerakines, P. A. 2016, ApJ, 827, 98
Luna, R., Millán, C., Domingo, M., Santonja, C., & Satorre, M. Á 2012, Vacuu, 86, 1969
Luna, R., Molpeceres, G., Ortigoso, J., et al. 2018, A&A, 617, A116
Luna, R., Satorre, M. Á, Santonja, C., & Domingo, M. 2014, A&A, 566, A27
Miller, T. M. 2009, in CRC Handbook of Chemistry and Physics, ed. D. R. Lide (89th ed.; Boca Raton, FL: CRC Press/Taylor and Francis)
Moore, M. H., & Hudson, R. L. 2010, in Proc. 2010 NASA Laboratory Astrophysics Workshop; October 25–28, 2010, Gatlinburg, TN, ed. D. R. Schultz (Athens, GA: Univ. Georgia), I20
Mousis, O., & Alibert, Y. 2006, A&A, 448, 771
Muñoz Caro, G. M., Ciaravella, A., Jiménez-Escobar, A., et al. 2019, ESC, 3, 2138
Newell, A. C., & Baird, R. C. 1965, JAP, 36, 3751
Orcutt, R. H., & Cole, R. H. 1967, JChPh, 46, 697
Panofsky, W. K. H., & Phillips, M. 1962, Classical Electricity and Magnetism (Boston, MA: Addison-Wesley)
Ramaswamy, K. L. 1935, Proc. Indian Acad. Sci., 2, 364
Roe, H. G., & Grundy, W. M. 2012, Icar, 219, 733
Romanescu, C., Marschall, J., Kim, D., Khatiwada, A., & Kalogerakis, K. S. 2010, Icar, 205, 695
Roux, J. A., Wood, B. E., Smith, M., & Plyfer, R. R. 1980, Infrared Optical Properties of Thin CO, NO, CH4, HC1, N2O, O2, AR, and Air Cryofilms, Arnold Engineering Development Center Int. Rep. AEDC-TR-79
Satorre, M. Á, Domingo, M., Millán, C., et al. 2008, P&SS, 56, 1748
Satorre, M. Á, Leliwa-Kopystynsky, J., Santonja, C., & Luna, R. 2013, Icar, 225, 703
Satorre, M. Á, Luna, R., Millán, C., Domingo, M., & Santonja, C. 2018, ASSL, 451, 51
Satorre, M. Á, Millán, C., Molpeceres, G., et al. 2017, Icar, 296, 179
Stone, J. M. 1963, Radiation and Optics (New York: McGraw-Hill)
Tempelmeyer, K. E., & Mills, D. W., Jr 1968, JAP, 39, 2968
Watson, H. E., Rao, G. G., & Ramaswamy, K. L. 1934, RSPSA, A143, 558
Wood, B. E., & Roux, J. A. 1982, JOSA, 72, 6
Yamagishi, M., Kaneda, H., Ishihara, D., et al. 2011, ApJL, 731, L20